forests

MDPI

Article

Soil Type, Topography, and Land Use Interact to Control the Response of Soil Respiration to Climate Variation

Chun Wang [1,2], Xiaoming Lai [1,2,*], Qing Zhu [1,2], Michael J. Castellano [3] and Guishan Yang [1,2]

1 Key Laboratory of Watershed Geographic Sciences, Nanjing Institute of Geography and Limnology, Chinese Academy of Sciences, 73 East Beijing Road, Nanjing 210008, China; springnju@aliyun.com (C.W.); qzhu@niglas.ac.cn (Q.Z.); gsyang@niglas.ac.cn (G.Y.)
2 University of Chinese Academy of Sciences, Beijing 100049, China
3 Department of Agronomy, Iowa State University of Science and Technology, Ames, IA 50011, USA; castelmj@iastate.edu
* Correspondence: xmlai@niglas.ac.cn; Tel.: +86-25-8688-2134

Received: 28 October 2019; Accepted: 4 December 2019; Published: 6 December 2019

check for updates

Abstract: The effects of soil and topography on the responses of soil respiration (R_s) to climatic variables must be investigated in the southeastern mountainous areas of China due to the rapid land-use change from forest to agriculture. In this study, we investigated the response of R_s to soil temperature (ST), precipitation over the previous seven days (AP7), and soil water content (SWC) across two hillslopes that had different land uses: a tea garden (TG) and a bamboo forest (BF). Meanwhile, the roles of soil properties including soil clay content and total nitrogen (TN), and topography including elevation, profile curvature (PRC), and slope on the different responses of R_s to these climatic variables were investigated. Results showed that mean R_s on the BF hillslope (2.21 umol C m^{-2} s^{-1}) was 1.71 times of that on the TG hillslope (1.29 umol C m^{-2} s^{-1}). Soil clay content, elevation, and PRC had negative correlations ($p < 0.05$) with spatial variation of R_s, and ST was positively correlated ($p < 0.01$) with temporal variation of R_s on both hillslopes. Across both hillslopes ST explained 33%–73% and AP7 explained 24%–38% of the temporal variations in R_s. The mean temperature sensitivities (Q_{10s}) of R_s were 2.02 and 3.22, respectively, on the TG and BF hillslopes. The Q_{10} was positively correlated ($p < 0.05$) with the temporal mean of SWC and TN, and negatively correlated ($p < 0.05$) with clay and slope. The mean AP7 sensitivities (a concept similar to Q_{10}) were greatly affected by clay and PRC. When R_s was normalized to that at 10 °C, power or quadratic relationships between R_s and SWC were observed in different sites, and the SWC explained 12%–32% of the temporal variation in R_s. When ST and SWC were integrated and considered, improved explanations (45%–81%) were achieved for the R_s temporal variation. In addition, clay and elevation had vital influences on the responses of R_s to SWC. These results highlight the influences of soil, topographic features, and land use on the spatial variations of the R_s, as well as on the responses of R_s to different climatic variables, which will supplement the understanding of controlling mechanisms of R_s on tea and bamboo land-use types in Southeastern China.

Keywords: greenhouse gas; mountainous area; soil respiration; Southeastern China

1. Introduction

The carbon dioxide (CO_2) released from soil respiration (R_s) is the second largest carbon flux in the terrestrial carbon cycle, only surpassed by CO_2 uptake through photosynthesis [1,2]. Hence, small changes in R_s rate may induce large changes in atmospheric CO_2 concentration [1]. Temporal and spatial variations of R_s are determined by the interactions of multiple environmental variables, including soil temperature (ST), precipitation, soil water content (SWC), vegetation cover, topography, and soil texture, etc. [3–6]. Therefore, to accurately predict the future changes in atmospheric CO_2 concentration, we must understand the response of R_s to environmental variables including potential feedbacks with future changes in climate and land use.

Responses of R_s to climatic variables including the ST, precipitation, and SWC and their interactions have been well documented in previous studies using field measurements, incubation experiments, model simulations, and a meta-analysis [3,7–9]. In general, the decomposition rate of soil organic matter—which accounts for ~50% of R_s—increases exponentially with ST [3,7,10]. However, high ST is often associated with low SWC. Liu et al. [11] found that at extremely high ST (e.g., >28 °C), R_s declined due to insufficient SWC. Carey et al. [12] reported a universal decline in the temperature sensitivity (Q_{10}) of R_s with ST > 25 °C, and this result may be due to low SWC at high ST. Precipitation influences R_s through two related mechanisms: one is stimulating the exchanges of substrates and gases in soil pores by rain dripping; the other is improving the connectivity of substrates through increasing SWC [11,13]. Generally, increased precipitation has a positive effect on R_s [8,13,14]. However, in regions with high precipitation inputs or soils with low water-holding capacity, increased precipitation can reduce the R_s because R_s declines at SWC exceeding field capacity due to slow diffusion of O_2 [11,15,16]. In contrast, in dry conditions, water in soil pores is disconnected, and dissolved organic C supply limits the metabolic activity of microbial communities [4,17]. Therefore, the relationship between SWC and R_s is typically quadratic, and the optimal SWC for R_s is near the field capacity due to the balance between substrate and O_2 diffusion [11,15,16,18].

Previous studies generally focused on the responses of R_s to the climatic variables, like ST, precipitation, and SWC at plot scales [8,13]. Despite these generalizations across regions within hillslope scales, soil properties and topographic features create great spatial heterogeneity [3,19] that change the spatial distribution of SWC, soil gas concentration, soil nutrients, and even the ST, and thus can induce the spatial heterogeneity of R_s [4,7]. By considering the effect of these spatial variables on the responses of R_s to the temporal variables (ST, precipitation, and SWC), there is a significant opportunity to improve our ability to predict and explain the response of R_s to land-use and climate changes [19].

The southeastern mountainous area occupies over 11.8% of the area of national land in China [20]. Much of this area suffers from intensive agricultural development, and tea plantations are a common vegetation type for the developed lands which have rapidly expanded in recent decades [21–23]. In this region, the expansion of tea plantations generally occurs at the expense of natural forested land like bamboo forest (BF) [24,25]. However, only few studies have investigated the feedback of R_s to the environmental variables in these two land-use types [21,26,27].

Here, we selected adjacent tea garden (TG) and bamboo forest (BF) hillslopes in the southeastern mountainous area of China as the study sites. The objectives of this study were to: (1) compare the temporal and spatial variations of R_s on these two hillslopes; (2) reveal the different responses of R_s to the ST, precipitation and SWC on these two hillslopes; and (3) determine the roles of soil properties and topographic features on the responses of R_s to the ST, precipitation, and SWC.

2. Materials and Methods

2.1. Study Hillslopes

The adjacent TG and BF hillslopes are located in the northern margin of the southeastern mountainous areas of China (31°21′N, 119°03′E) (Figure 1). The vegetation types on the TG and BF hillslopes were green tea (*Camellia sinensis* (L.) O. Kuntze) and Moso bamboo (*Phyllostachys edulis* (Carr.) H. de Lehaie), respectively. The region has a subtropical monsoon climate and the annual mean temperature and precipitation over the period from 2006 to 2016 were 1157 mm and 15.9 °C, respectively. The foot of the hillslope was near a pond. Lai et al. [28] provides detailed descriptions of the soil and topographic features of the TG and BF hillslopes.

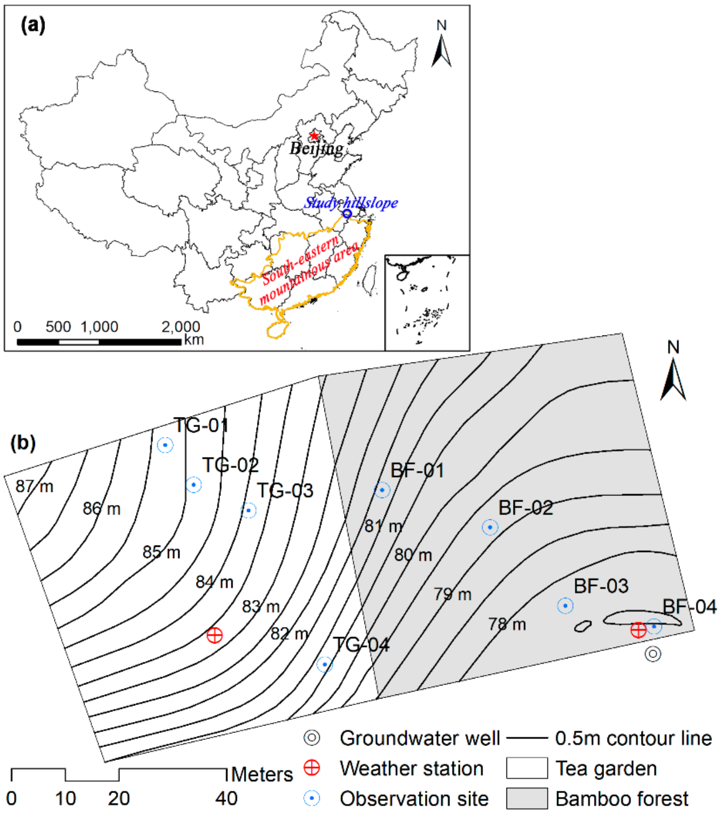

Figure 1. (**a**) The geographic location of the tea garden (TG) and bamboo forest (BF) hillslopes in the southeastern mountainous areas of China, and (**b**) the spatial distributions of the observation sites and weather stations as well as the groundwater well on the study hillslopes.

The TG hillslope was planted with green tea for ~15 years, replacing from bamboo forest, while the BF hillslope was un-managed for >35 years. Fertilizers were applied twice per year on the TG hillslope: spring fertilizer applied in March (urea: 209 kg N ha^{-1}), and basal fertilizer was applied in October (urea: 174 kg N ha^{-1}; organic fertilizer: 1792 kg C ha^{-1} and 120 kg N ha^{-1}). Tea leaf was pruned in May every year, and left on the soil surface. No fertilizer or tillage was applied on the BF hillslope.

2.2. Data Collection

Four observation sites were respectively allocated along the slope transects on the TG and BF hillslopes (TG-01, TG-02, TG-03, and TG-04; BF-01, BF-02, BF-03, and BF-04) (Figure 1b). Paired EC-5 and MPS-6 sensors (Decagon Devices Inc., Pullman WA, USA) were installed at 10-cm depths at these observation sites to measure SWC and ST. Before sensor installation, at all observations sites, soil samples were collected from depths of 0–20 cm. After being dried, weighted, ground, and sieved through a 2-mm polyethylene sieve, contents of clay (<0.002 mm), silt (0.002–0.05 mm), and sand (0.05–2 mm), soil organic carbon (SOC), and total nitrogen (TN) were then measured. The soil samples were collected in October, long after the application of spring fertilizer and just before the basal fertilization to minimize effects of inorganic nutrient inputs on SOC and TN. Thus, these measured SOC and TN values could be considered the initial SOC and TN values on the TG and BF hillslopes. The depth to bedrock (DB) was measured in excavated soil profiles. In addition, the topographic features including elevation, slope, and profile curvature (PRC) at these observation sites were extracted from a local elevation survey with 1-m spatial resolution. Weather stations (Decagon Devices Inc., Pullman WA, USA) were installed on the TG and BF hillslopes to record precipitation under the canopies. All these measurements including ST, SWC, and precipitation were collected with a frequency of 5 min.

Soil properties and topographic features at observation sites of the TG and BF hillslopes were presented in Table 1.

Table 1. Soil and topographic properties of the four observation sites on the tea garden (TG) and bamboo forest (BF) hillslopes. DB: depth to bedrock; SOC: soil organic carbon content; TN: soil total nitrogen content; PRC: profile curvature. The percentages of sand, silt, clay, SOC, and TN were defined by weight.

Properties	TG Hillslope				BF Hillslope			
	TG-01	TG-02	TG-03	TG-04	BF-01	BF-02	BF-03	BF-04
Sand (%)	10.28	12.27	8.39	13.3	19.24	15.85	5.96	6.26
Silt (%)	75.86	71.22	71.71	71.99	68.5	71.26	81.71	82.02
Clay (%)	13.86	16.51	19.90	14.71	12.26	12.89	12.33	11.72
DB (cm)	41.07	40.32	41.73	58.12	28.27	86.12	59.08	71.12
SOC (%)	1.32	1.43	0.96	0.76	1.24	1.35	1.40	1.47
TN (%)	0.13	0.13	0.08	0.07	0.12	0.14	0.15	0.14
Elevation (m)	86.03	85.14	83.8	80.71	81.36	79.14	77.63	77.5
Slope (%)	9.59	9.28	12.84	17.92	15.99	8.31	5.27	0.22
PRC	−0.28	1.63	2.93	−0.21	−8.21	−1.00	−0.76	0.00

Gas sampling was performed between 09:00 and 11:00 h from 13 April 2016 to 22 March 2018, with a frequency of once or twice a month (a total of 28 times). Around each observation site, three closed chambers were installed to collect the gas samples with a space of 0.50 m between each other. Thus three replicates of gas samples could be obtained for one site. At each chamber, gas samples were collected at 0, 10, 20, and 30 min after chamber closure, and the CO_2 and N_2O concentrations in each gas samples were analyzed using a gas chromatograph (7890B, Agilent Technologies, Santa Clara, CA, USA). The measurements of R_s (CO_2 emission flux) and N_2O emission flux were described in detail by Fu et al. [23] and Liao et al. [29], respectively.

In addition, three zero-tension lysimeters were also installed around each observation site to collect the soil leachates of up to 30 cm in depth. Soil leachate samples were collected at the gas sampling date and were filtered through 0.45-mm paper. The NO_3^--N and total organic carbon (TOC) concentrations in leachates were measured respectively using the continuous flow analyzer (San^{++}, Skalar, Breda, The Netherlands) and the total organic carbon analyzer (Torch, Teledyne Tekmar, Cincinnati, Ohio, USA). In addition, around each site, three soil samples at 0–20 cm soil depths were collected at the same date with gas and leachate sampling, and the soil NO_3^--N and NH_4-N concentrations were determined by extracting with 2 mol L^{-1} KCl solution. The averaged R_s, N_2O emission flux, leachate NO_3^--N and TOC concentrations, and soil NO_3^--N and NH_4-N concentrations of three replicates for each site were used as the final measurements. The ground water table depth at each site was calculated on each sampling date, based on the difference between the elevation of each site and the ground water table depth measured in the groundwater well (Figure 1b).

2.3. Data Analysis

One-way analysis of variance with Tukey's HSD test was used to test the differences of different variables among different observation sites and on the TG and BF hillslopes. Statistical significance was identified at the 0.05 level. Correlation analyses were conducted to investigate the relationships between R_s and soil N_2O emission flux, leachate NO_3^--N and TOC concentrations, soil NO_3^--N content, SWC, ST, groundwater table depth, and the antecedent precipitation. The cumulative antecedent precipitation amount during previous the 7 days (AP7) was used as the antecedent precipitation, as better correlations were found between R_s and AP7 as compared to using smaller day length for calculating the antecedent precipitation.

An exponential function was used to explore the relationship between R_s and ST at a 10–cm depth:

$$R_s = \alpha \times e^{\beta \times ST} \quad (1)$$

where α, β are coefficients fitted by the least-square method.

The temperature sensitivity Q_{10}, described as a proportional change in R_s with a 10 °C increase in temperature, was calculated by:

$$Q_{10} = e^{10\times\beta} \tag{2}$$

Similarly, an exponential function was also used to detect the relationship between R_s and AP7, and precipitation sensitivity P_{10}, was proposed as a proportional change in R_s with a 10-mm increase in AP7:

$$R_s = m \times e^{n\times AP7} \tag{3}$$

$$P_{10} = e^{10\times n} \tag{4}$$

The R_s was normalized to 10 °C (R_{s10}) to minimize the effect of ST and investigate the relationship with the SWC at a 10-cm depth:

$$R_{s10} = R_s \times e^{\beta\times(10-ST)} \tag{5}$$

where β is the coefficient derived from Equation (1).

Power and quadratic functions were used to explore the relationship between R_{s10} and the SWC, and the fitted function with best accuracy was selected.

To detect the relationships between R_s and the interactions of ST and SWC, two-factor regression model analyses were performed as follows:

$$R_s = a + b \times ST + c \times SWC \tag{6}$$

$$R_s = a \times ST^b \times SWC^c \tag{7}$$

$$R_s = a \times e^{b\times ST} \times SWC^c \tag{8}$$

where *a*, *b*, *c* are coefficients fitted by the least-square method.

Spearman rank correlation analyses were conducted to investigate the relationships between the temporal mean R_s, Q_{10}, P_{10}, coefficient *c* in Equations (6), (7), and (8), spatial variables including soil texture, DB, SOC, TN, elevation, slope, and PRC, and temporal mean SWC and ST. All statistical analyses were conducted with SPSS 18.0 (SPSS Inc., Chicago, IL, USA) or Origin Pro 8.5 (OriginLab, Northampton, MA, USA).

3. Results

3.1. Differences in Environmental Variables on TG and BF Hillslopes

Soil properties and topographic features differed among the observation sites on the TG and BF hillslopes (Table 1). Among the eight sites, greater sand contents were found in BF-01 and BF-02, while BF-03 and BF-04 had greater contents of silt. The TG-03 site also had lower sand content and greater clay content among these sites. Relative to the TG hillslope, the clay content on the BF hillslope was lower. Deeper soil depths (i.e., DB) were observed on the BF hillslope, while the shallowest soil depth was found in BF-01. The initial soil SOC and TN values were slightly greater on the BF hillslope than on the TG hillslope. The elevation of BF hillslope was generally lower than that on the TG hillslope. Greater slope was found in the TG-03, TG-04, and BF-01 sites, while the TG-01, TG-02, and BF-02 sites had a medium slope, and the BF-04 site had the gentlest slope. The positive PRC were found in TG-02 and TG-03, which indicated a convergent terrain, while the PRC in TG-01, TG-04, BF-01, BF-02, and BF-03 were negative, which indicated a divergent terrain.

Soil N_2O emission flux, leachate NO_3^--N and TOC concentrations, soil NO_3^--N, water contents, and temperature at a 10-cm depth also differed among observation sites on the TG and BF hillslopes (Table 2 and Figure 2). Soil N_2O emission flux, leachate NO_3^--N and TOC concentrations, and soil NO_3^--N content were significantly greater ($p < 0.05$) on the TG hillslope than on the BF hillslope (Table 2). Mean soil N_2O flux, leachate NO_3^--N and TOC concentrations, and soil NO_3^--N content on the TG hillslope were respectively 3.25, 4.29, 1.66, and 1.55 times of those on the BF hillslope. The greatest soil N_2O flux, leachate NO_3^--N concentration, and soil NO_3^--N content were found in TG-03. The ST at 10-cm depths were similar between the TG and BF hillslopes ($p > 0.05$), while slightly higher ST was observed on the TG hillslope during warm seasons and on the BF hillslope during cooler seasons (Figure 2a). The SWC at 10-cm depths on the TG hillslope was significantly lower ($p < 0.05$) than that on the BF hillslope (Table 2). The mean SWC on the TG hillslope was 0.72 times of that on the BF hillslope (Figure 2b). Significant correlations ($r > 0.43$, $p < 0.05$) between SWC and AP7 were observed on the TG hillslope, while the correlations were non-significant ($r < 0.31$, $p > 0.05$) on the BF hillslope. In addition, the ground water table depth in BF-04 ranged from 0.18 to 1.10 m (Figure 2). The temporal variations of ground water table depth were opposite to those of the SWC; a low SWC and a deep ground water table were observed from July to September 2016 and from November to December 2017 (Figure 2). The ground water table was shallow in BF-03 and BF-04, which caused the high SWC in these two sites (Table 2).

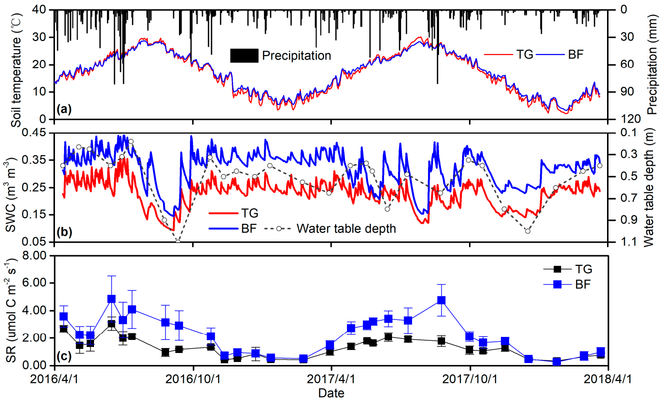

Figure 2. Temporal variations of (**a**) the mean soil temperature at 10-cm depths of the observation sites on the tea garden (TG) and bamboo forest (BF) hillslopes; (**b**) the mean soil water content (SWC) on the TG and BF hillslopes and the water table depth at site BF-04; and (**c**) the mean soil respiration (SR) on the TG and BF hillslopes. The error bar represents the standard deviation.

Table 2. Statistical summaries of the soil respiration rate (i.e., CO_2 flux) and N_2O emission flux, leachate NO_3^--N and total organic carbon (TOC) concentrations, soil NO_3^--N content, soil water content (SWC), and soil temperature (ST) at 10-cm soil depths. Statistical summaries of the measured data at different observation sites and on hillslopes with different land uses are shown by the means ± standard deviations. One-way ANOVA and Tukey's test were used to compare the data among different observation sites and hillslopes with different land uses. Different letters indicate significant differences at the $p < 0.05$ level.

Site	*Gas Emission*		*Leachate*		*Soil*		
	CO_2 umol C m^{-2} s^{-1}	**N_2O g N ha^{-1}**	**NO_3^--N mg N L^{-1}**	**TOC mg C L^{-1}**	**NO_3^--N mg N kg^{-1}**	**ST °C**	**SWC m^3 m^{-3}**
TG-01	1.25 ± 0.7^{a}	6.3 ± 8.7^{bcd}	13.7 ± 6.5^{bc}	31.0 ± 14.3^{cd}	24.3 ± 14.5^{ab}	16.9 ± 7.3^{a}	0.16 ± 0.03^{a}
TG-02	1.35 ± 0.8^{a}	7.2 ± 9.1^{cd}	17.7 ± 9.0^{c}	36.6 ± 14.9^{d}	21.6 ± 16.5^{ab}	16.9 ± 7.2^{a}	0.25 ± 0.05^{b}
TG-03	1.22 ± 0.7^{a}	7.9 ± 9.1^{d}	16.0 ± 8.7^{c}	15.3 ± 9.7^{a}	29.7 ± 30.3^{b}	16.9 ± 7.5^{a}	0.35 ± 0.06^{d}
TG-04	1.35 ± 0.7^{a}	4.4 ± 6.6^{abcd}	10.8 ± 6.1^{b}	24.8 ± 10.9^{bc}	16.6 ± 25.6^{ab}	16.8 ± 6.2^{a}	0.15 ± 0.04^{a}
BF-01	2.27 ± 1.4^{bc}	1.1 ± 0.7^{a}	3.7 ± 2.6^{a}	19.1 ± 9.2^{ab}	17.9 ± 21.4^{ab}	16.7 ± 6.6^{a}	0.22 ± 0.06^{b}
BF-02	2.45 ± 1.5^{c}	1.9 ± 1.0^{ab}	4.3 ± 2.4^{a}	13.6 ± 6.1^{a}	16.9 ± 13.4^{ab}	16.8 ± 6.4^{a}	0.30 ± 0.07^{c}
BF-03	2.54 ± 1.7^{c}	2.8 ± 2.0^{abc}	3.5 ± 2.9^{a}	17.0 ± 7.1^{a}	15.8 ± 11.7^{ab}	17.4 ± 6.4^{a}	0.37 ± 0.06^{d}
BF-04	1.57 ± 1.0^{ab}	2.1 ± 1.5^{ab}	2.2 ± 1.6^{a}	15.1 ± 7.0^{a}	9.2 ± 6.0^{a}	16.8 ± 5.5^{a}	0.39 ± 0.09^{d}
Land use							
TG	1.29 ± 0.7^{A}	6.5 ± 8.5^{B}	14.6 ± 8.0^{B}	26.9 ± 14.8^{B}	23.1 ± 22.9^{B}	16.9 ± 7.0^{A}	0.23 ± 0.10^{A}
BF	2.21 ± 1.3^{B}	2.0 ± 1.5^{A}	3.4 ± 2.5^{A}	16.2 ± 7.6^{A}	14.9 ± 14.5^{A}	16.9 ± 6.2^{A}	0.32 ± 0.09^{B}

3.2. Spatial and Temporal Variations of R_s

The R_s varied among observation sites and on the TG and BF hillslopes (Table 2). The greatest R_s was found in BF-03 (2.54 umol C m^{-2} s^{-1}), and a relatively greater R_s was also found in BF-01 and BF-02 (>2.25 umol C m^{-2} s^{-1}). However, small and similar amounts of R_s were found in TG-01, TG-02, TG-03 and TG-04 (1.22–1.35 umol C m^{-2} s^{-1}). The R_s on the BF hillslope was significantly higher ($p < 0.05$) than that on the TG hillslope (the mean R_s on BF hillslope was 1.71 times of that on the TG hillslope). The temporal variations of the R_s both on the TG and BF hillslopes were generally in accordance with the temporal changes of the measured ST at 10 cm depths (Figure 2). The R_s ranged from 0.34 to 3.06 umol C m^{-2} s^{-1} on the TG hillslope, and from 0.25 to 4.84 umol C m^{-2} s^{-1} on the BF hillslope during the observation period. When a higher R_s was observed, greater differences between the mean R_s on the TG and BF hillslope were observed (Figure 2). Greater spatial variations of R_s among observation sites could be found on the BF hillslope due to relatively low R_s in BF-04. The standard deviations (SD) of R_s ranged from 0.01 to 0.56 umol C m^{-2} s^{-1} on the TG hillslope, and from 0.06 to 1.67 umol C m^{-2} s^{-1} on the BF hillslope (Figure 2).

3.3. Relationships between R_s and Environmental Variables

Soil clay content, elevation, and PRC were all negatively correlated ($r = -0.71$, -0.74 and -0.74, respectively, $p < 0.05$) with R_s. There was also a positive relationship between R_s and TN ($r = 0.64$, $p = 0.09$), while low r values (absolute value of $r < 0.45$) were found between R_s and sand, DB, SOC, slope, temporal mean SWC, and ST.

Correlations between temporal variations in R_s and the temporal factors varied among different observation sites and on the TG and BF hillslopes (Table 3). Both N_2O flux and ST were positively correlated ($p < 0.05$) with the mean R_s on the TG and BF hillslopes. The r value between R_s and ST was great (>0.70) in all observation sites and on the TG and BF hillslopes. The r values between R_s and N_2O flux and ST were greater on the BF hillslope than on the TG hillslope. Likewise, positive correlations ($p < 0.05$) were found between R_s and leachate TOC concentration and AP7 on the BF hillslope, while no such relationship was found on the TG hillslope. Specifically, significant correlations ($p < 0.05$) between R_s and leachate TOC concentration were found in BF-01 and BF-04, while significant correlations ($p < 0.05$) between R_s and AP7 were found in BF-01 and BF-02. Positive correlations between R_s and AP7 were significant ($p < 0.05$) in TG-01 and TG-04. In addition, the negative correlation between R_s and leachate NO_3^--N concentration was significant ($p < 0.05$) on the TG hillslope, but non-significant on the BF hillslope. In general, correlations between R_s and soil NO_3^--N content, SWC, and ground water table depth were non-significant ($p > 0.05$).

Table 3. Correlation coefficients between the soil respiration and ancillary variables at different observation sites on the tea garden (TG) and bamboo forest (BF) hillslopes. Ancillary variables included soil N_2O emission flux, leachate NO_3^--N and total nitrogen carbon (TOC) concentrations, soil NO_3^--N content, soil water content (SWC), soil temperature (ST) at 10-cm depths, groundwater table depths (GWTD), and the antecedent precipitation during previous 7 days (AP7).

Site	N_2O Flux	Leachate		Soil			GWTD	AP7
		NO_3^-–N	TOC	NO_3^-–N	SWC	ST		
TG-01	0.337	−0.493 *	−0.145	0.300	0.243	0.708 **	−0.338	0.378 *
TG-02	0.362	−0.463 *	−0.040	0.384 *	0.015	0.720 **	−0.343	0.361
TG-03	0.444 *	−0.255	−0.069	0.072	0.083	0.722 **	−0.131	0.224
TG-04	0.234	−0.438 *	0.054	−0.035	0.368	0.630 **	−0.211	0.389 *
BF-01	0.525 **	−0.338	0.401 *	0.208	−0.225	0.844 **	−0.242	0.516 **
BF-02	0.620 **	−0.473 *	0.254	−0.029	−0.122	0.877 **	−0.227	0.474 *
BF-03	0.453 *	−0.005	0.388	−0.120	−0.285	0.858 **	0.101	0.302
BF-04	0.407 *	0.133	0.447 *	−0.410 *	−0.376 *	0.817 **	0.022	0.348
Land use								
TG	0.379 *	−0.425 *	−0.081	0.184	0.218	0.734 **	−0.273	0.357
BF	0.571 **	−0.240	0.399 *	−0.022	−0.263	0.895 **	−0.091	0.431 *

Note. The symbols of * and ** denote significant correlations at $p < 0.05$ and $p < 0.01$, respectively.

4. Discussion

4.1. Factors Influencing R_s response to ST

The ST at 10-cm depth explained 33%–45% and 59%–73% of the temporal variations in R_s on the TG and BF hillslopes, respectively, using the exponential functions (Figure 3). The temporal trends of R_s were mainly controlled by ST, which were consistent with many previous studies [3,7,10]. However, the exponential relationships between ST and R_s were poor when ST was high, especially on the TG hillslope (Figure 3). This was because when ST was low, the R_s was mainly constrained by ST, while under high ST conditions, other environmental variables like the SWC and substrate supplies would have a great influence on R_s [3]. Because of the lower SWC on the TG hillslope, the R_s was more likely to be constrained by SWC under high ST conditions, especially in TG-04 with the lowest SWC (Table 2). This result was consistent with that of Liu et al. [11] and Carey et al. [12]. Li et al. [3] also indicated that when the R_s values from the days with extreme low SWC were discarded, the explanation rates of ST on R_s increased.

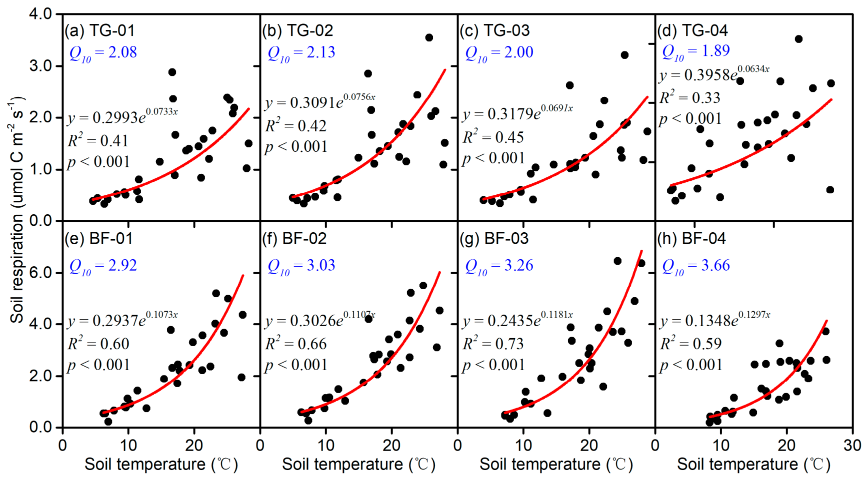

Figure 3. Exponential relationships between soil respiration and soil temperature at a 10-cm depth at different observation sites on the tea garden hillslope and bamboo forest hillslope. The Q_{10} is the temperature sensitivity of soil respiration.

The mean Q_{10} was 2.02 on the TG hillslope and ranged from 1.89 to 2.13, lower than that on the BF hillslope (mean Q_{10}: 3.22, range from 2.92 to 3.66) (Figure 3). The Q_{10} on the TG hillslope in our study was consistent with that observed in Zhejiang, China (range from 1.86 to 1.98) [30], greater than that observed in Sichuan, China (range from 1.15 to 1.40) [31], and lower than that observed in Yunnan, China (5.7) [32]. In addition, the Q_{10} of the BF hillslope was a little higher than that observed in a BF in Zhejiang, China (2.80) [26], and lower than that observed in a BF in central Taiwan, China (4.09) [33]. The different Q_{10} on the TG and BF hillslopes derived from this study and the other studies might be attributed to the different soil water availability, temperature range, substrate quality, or microbial community [34].

The lower Q_{10} on the TG hillslope relative to that on the BF hillslope might be due to lower initial soil C and N contents and higher soil clay content (Table 1). Positive correlations between Q_{10} and TN ($r = 0.88$, $p < 0.01$), temporal mean SWC ($r = 0.74$, $p < 0.05$), and negative correlations between Q_{10} and clay ($r = –0.81$, $p < 0.05$), slope ($r = –0.86$, $p < 0.01$) were observed in this study. Higher initial soil C and N availability induced abundant microbial communities and enhanced soil enzyme activities, which was highly related to the R_s as well as Q_{10} [35]. Although excess N fertilizer was applied on the TG hillslope (Table 2), this would not substantially improve the soil microbial communities due to the N consumption by tea plantation and high N losses through gas and solute pathways (Table 2). In addition, excess inorganic N fertilization tended to suppress microbial activities, as revealed by Mahal et al. [36]. A positive relationship between Q_{10} and SWC was found by Flanagan and Johnson [37] and Zhou et al. [38], while a negative correlation or no effect were found in other studies [6,39,40]. One of the reasons for this might be whether the observed ranges of SWC covered the optimum SWC for R_s (near to field capacity) [15,18]. Previous studies have indicated the inhibition effects of clay on R_s by impeding mineralization of soil organic matter, and thus posed negative on Q_{10} [4,41]. In addition, large slope was always companied by low soil water and nutrient-holding capacities [19], which would result in low R_s and the negative effects on Q_{10}.

4.2. Factors Influencing R_s Response to Precipitation

Relationships between R_s and AP7 could also be described by the exponential functions in this study (Figure 4). The AP7 explained 24%–37% (mean: 31%) and 28%–38% (mean: 35%) of the temporal variations in R_s on the TG and BF hillslopes, respectively. Positive relationships between R_s and precipitation were also found by Chen et al. [13] and Zhou et al. [8], while some other studies demonstrated that increased precipitation could reduce R_s due to the slow gas diffusion [15,42]. In this study, the relative lower explanation rates (<30%) of AP7 on R_s in TG-03, BF-03, and BF-04 were due to the wet soil conditions at these sites (Table 2). This confirmed the inhibition effects of high SWC on the responses of R_s to AP7. In addition, negative correlations between clay ($r = -0.82$, $p < 0.05$), PRC ($r = -0.79$, $p < 0.05$) and P_{10} also indirectly confirmed the inhibition effects. High clay content was always associated with high water-holding capacity [43], and large PRC represented the depressions where it was easy to accumulate water [44], inducing a low sensitivity of R_s to precipitation.

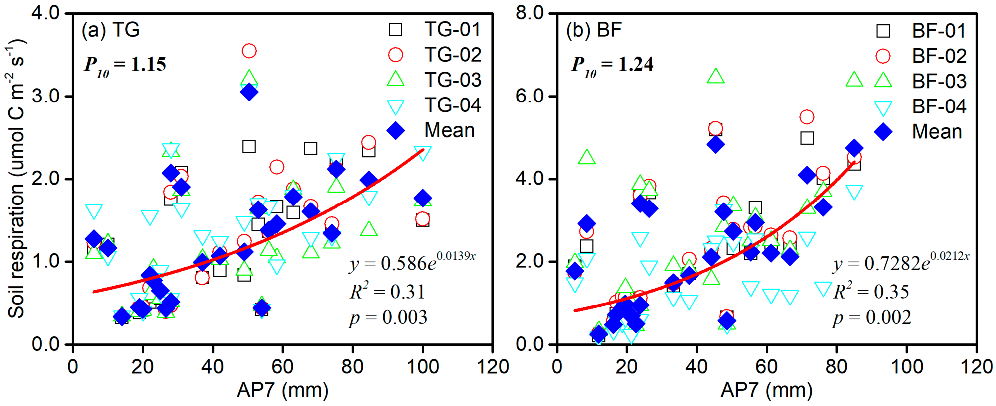

Figure 4. Relationships between soil respiration at the observation sites on the (**a**) tea garden (TG) and (**b**) bamboo forest (BF) hillslopes and their corresponding antecedent precipitation during previous 7 days (AP7). The exponential correlations between the spatial mean values and the AP7 are also shown. The P_{10} is the precipitation sensitivity of soil respiration.

4.3. Factors Influencing R_s Response to SWC

In this study, correlations between R_s and SWC were relatively poor (Table 3). However, when R_s was normalized to that at 10 °C, power relationships between R_s and SWC were observed in TG-01, TG-02, TG-04, and quadratic relationships were observed in TG-03, BF-01, BF-02, and BF-04, while an ambiguous power relationship was found in BF-03 (Figure 5). The SWC explained 12%–32% of the temporal variations of R_s except in BF-03 (Figure 5). The different curves fitting the relationships between SWC and R_s could be attributed to the different ranges of SWC observed in these sites. The quadratic relationships between SWC and R_s have been demonstrated by previous studies including those of Liu et al. [11], Hursh et al. [9], and Han et al. [15]. The optimum SWC for R_s was near the field capacity [15,18]. Therefore, when the observed SWC was below the optimum value (e.g., TG-01, TG-02, and TG-04), only positive power relationships between SWC and R_s could be extracted. When the observed SWC covered the optimum value (e.g., TG-03, BF-01, BF-02, and BF-04), the quadratic relationships could be captured. In BF-03, as the observed SWC was kept around the optimum value; thus, an ambiguous negative power relationship was observed, and also the largest mean R_s was found (Table 2).

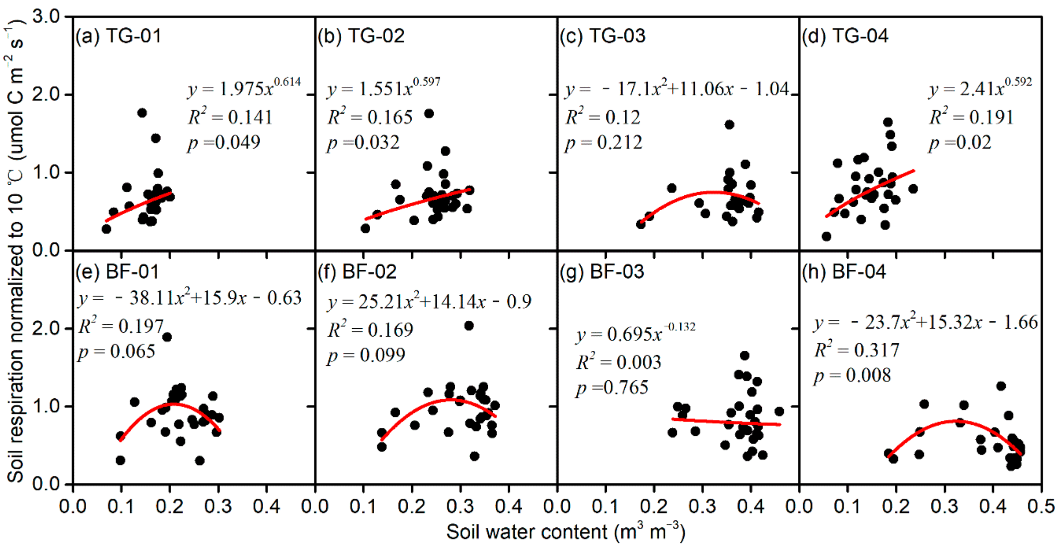

Figure 5. Power or quadratic relationships of the soil respiration normalized to 10 °C with the soil water content at a 10-cm depth of the observation sites on the tea garden (TG) and bamboo forest (BF) hillslopes.

In order to extract the combined effect of ST and SWC on R_s, we integrated both ST and SWC into three two-factor regression models (Equations (6)–(8)). The ST and SWC together explained 45%–81% of the temporal variations in R_s in different observation sites and on the TG and BF hillslopes, with a relatively higher explanation rate acquired by Equation (7) (Table 4). The combined effects of ST and SWC on R_s temporal variations were consistent with previous studies [3,7,11], which also reported better explanation rates with these two-factor regression models than with one-factor regression models. In addition, for large spatial scales, previous studies also indicated that ST alone was insufficient to accurately predict the R_s, and that other factors such as SWC or TN should be considered also [6,7].

Table 4. Fitted Equations (6), (7), and (8) of soil respiration (R_s) against soil temperature (ST) and soil water content (SWC) in different observation sites and on tea garden (TG) and bamboo forest (BF) hillslopes, with the corresponding determination coefficients (R^2). In these equations, *a*, *b*, *c* are coefficients fitted by the least-square method.

Site	**Equation (6)** $R_s = a + b\mathrm{ST} + c\mathrm{SWC}$	R^2	**Equation (7)** $R_s = a\mathrm{ST}^b\,\mathrm{SWC}^c$	R^2	**Equation (8)** $R_s = ae^{b\mathrm{ST}}\,\mathrm{SWC}^c$	R^2
TG-01	$R_s = -0.977 + 0.073\mathrm{ST} + 6.427\mathrm{SWC}$	0.57	$R_s = 0.262\mathrm{ST}^{0.986}\,\mathrm{SWC}^{0.650}$	0.60	$R_s = 1.741e^{0.057\mathrm{ST}}\,\mathrm{SWC}^{0.729}$	0.55
TG-02	$R_s = -0.989 + 0.087\mathrm{ST} + 3.546\mathrm{SWC}$	0.56	$R_s = 0.125\mathrm{ST}^{1.124}\,\mathrm{SWC}^{0.559}$	0.60	$R_s = 1.051e^{0.065\mathrm{ST}}\,\mathrm{SWC}^{0.652}$	0.56
TG-03	$R_s = -0.826 + 0.072\mathrm{ST} + 2.333\mathrm{SWC}$	0.56	$R_s = 0.110\mathrm{ST}^{1.055}\,\mathrm{SWC}^{0.546}$	0.59	$R_s = 0.793e^{0.062\mathrm{ST}}\,\mathrm{SWC}^{0.663}$	0.56
TG-04	$R_s = -0.478 + 0.069\mathrm{ST} + 4.607\mathrm{SWC}$	0.48	$R_s = 0.235\mathrm{ST}^{0.953}\,\mathrm{SWC}^{0.484}$	0.54	$R_s = 1.468e^{0.055\mathrm{ST}}\,\mathrm{SWC}^{0.550}$	0.52
BF-01	$R_s = -1.667 + 0.194\mathrm{ST} + 3.165\mathrm{SWC}$	0.72	$R_s = 0.055\mathrm{ST}^{1.538}\,\mathrm{SWC}^{0.419}$	0.76	$R_s = 0.998e^{0.086\mathrm{ST}}\,\mathrm{SWC}^{0.477}$	0.72
BF-02	$R_s = -2.230 + 0.215\mathrm{ST} + 3.596\mathrm{SWC}$	0.79	$R_s = 0.048\mathrm{ST}^{1.556}\,\mathrm{SWC}^{0.404}$	0.81	$R_s = 0.899e^{0.087\mathrm{ST}}\,\mathrm{SWC}^{0.454}$	0.77
BF-03	$R_s = -0.693 + 0.225\mathrm{ST} - 1.840\mathrm{SWC}$	0.74	$R_s = 0.014\mathrm{ST}^{1.750}\,\mathrm{SWC}^{-0.117}$	0.75	$R_s = 0.411e^{0.093\mathrm{ST}}\,\mathrm{SWC}^{-0.042}$	0.74
BF-04	$R_s = -0.107 + 0.140\mathrm{ST} - 1.760\mathrm{SWC}$	0.69	$R_s = 0.017\mathrm{ST}^{1.555}\,\mathrm{SWC}^{-0.077}$	0.66	$R_s = 0.318e^{0.087\mathrm{ST}}\,\mathrm{SWC}^{-0.033}$	0.62
Land use						
TG	$R_s = -0.073 + 0.074\mathrm{ST} + 0.520\mathrm{SWC}$	0.49	$R_s = 0.121\mathrm{ST}^{0.941}\,\mathrm{SWC}^{0.176}$	0.51	$R_s = 0.676e^{0.053\mathrm{ST}}\,\mathrm{SWC}^{0.196}$	0.46
BF	$R_s = -0.667 + 0.191\mathrm{ST} - 1.128\mathrm{SWC}$	0.68	$R_s = 0.024\mathrm{ST}^{1.616}\,\mathrm{SWC}^{0.077}$	0.68	$R_s = 0.501e^{0.088\mathrm{ST}}\,\mathrm{SWC}^{0.115}$	0.65

The coefficient *c* of SWC in Equations (6)–(8) was negative in BF-03 and BF-04, and positive in other observation sites, which indicated the general inhibition effects of SWC in BF-03 and BF-04, and promotion effects in other sites (Table 4). This also could be approximately reflected in Figure 5. Negative relationships ($r = -0.86$, $p < 0.01$) were observed between SWC and the coefficient *c* in Equation (6), which indicated that the influences of SWC on R_s always ranged from promotion (positive) to inhibition (negative) with the increasing of SWC [4,15]. In addition, both clay ($r = 0.71$ and 0.74, respectively, $p < 0.05$) and elevation ($r = 0.95$ and 0.93, respectively, $p < 0.01$) were positively correlated with the coefficient *c* in Equations (7) and (8). Clay improved the soil water-holding capacity and prevented soil organic matters from decomposition [41,43], and thus the dependence of R_s on the ST declined and the importance of SWC increased. Elevation determined the depth to groundwater level in different observation sites, and thus indirectly altered the SWC. Regions with high elevation were always featured by dry soil condition, this resulted in the great dependence of R_s on SWC.

4.4. Relation between Land Use and R_s

Land use was recognized as one key factor determining the spatial variations of R_s [6,30,34]. In addition, land-use change from natural forestland to agricultural land has been a common phenomenon in the mountainous area in recent decades [25,45]. Different root biomass and exudates between the forestland and agricultural land determined the differences of the characteristics of root autotrophic respiration and the rhizosphere condition; the latter could change soil microbial community compositions [13,34]. In addition, the intensive human management of agricultural land, including fertilization and tillage, could change soil conditions like soil structure and soil C and N availability. The changes of soil condition thus could affect the root autotrophic respiration and change the soil microbial communities and activities, which directly determined the soil heterotrophic respiration [34]. In this study, higher R_s and Q_{10} were observed on the BF hillslope than on the TG hillslope (Table 2 and Figure 3). Reasons for the higher R_s on the BF hillslope were identified as the higher soil water content and C and N availabilities in this study. High soil water content and C and N availabilities could enhance the root and microbial activities and respiration [19]. However, the direct factors of soil microbial community compositions as well as the root respiration properties were not investigated in this study, and need to be considered to reveal the relationship between land use and R_s in further work.

5. Conclusions

In this study, responses of R_s to the ST, precipitation, and SWC and their relationship with soil and terrain properties were investigated in different observation sites and among different land-use types. The mean R_s on the BF hillslope was 2.21 umol C m^{-2} s^{-1}, significantly larger than that on the TG hillslope (1.29 umol C m^{-2} s^{-1}) during the observation period. Spatial variations of R_s were negatively correlated ($p < 0.05$) with clay, elevation, and PRC. Temporal variations of R_s were correlated ($p < 0.05$) with ST and soil N_2O flux on both the TG and BF hillslopes. The ST was the dominant temporal factor of the R_s, and explained 33%–45% and 59%–73% of the R_s, on TG and BF hillslopes, respectively. The mean Q_{10} on the TG hillslope was 2.02, which was lower than that on the BF hillslope (mean: 3.22). Positive correlations ($p < 0.05$) were found between Q_{10} and TN and SWC, and negative correlations ($p < 0.05$) were found between Q_{10} and clay and slope. The AP7 explained 24%–37% and 28%–38% of the R_s on the TG and BF hillslopes, respectively, and both clay and PRC were significantly negatively correlated ($p < 0.05$) with P_{10} (a proportional change in R_s with a 10-mm increase in AP7). Power or quadratic relationships between R_s and SWC were detected in different sites, and the SWC explained 0%–32% of the temporal variations of R_s. Improved explanation rates (45%–81%) were achieved when both ST and SWC were considered together in the two-factor regression models. The temporal mean SWC, clay, and elevation had great influences ($p < 0.05$) on the dependencies of R_s on SWC. The study highlights the roles of soil and topographic features in inducing the spatial variations of R_s and the responses of R_s to climatic variables in the mountainous area. These results can supplement the knowledge of response mechanisms of R_s to different climatic variables on TG and BF hillslopes, facilitating modelling prediction of R_s at large scales.

Author Contributions: Conceptualization, C.W., X.L., and Q.Z.; Data curation, C.W. and X.L.; Formal analysis, C.W. and X.L.; Methodology, C.W., X.L., and Q.Z.; Writing—original draft, C.W. and X.L.; Writing—review and editing, X.L., Q.Z., and M.J.C.; Supervision, G.Y.

Funding: This study was funded by the National Natural Science Foundation of China, grant number (41901030), the Key Research Program of Frontier Sciences, Chinese Academy of Sciences, grant number (QYZDB-SSW-DQC038), and the Natural Science Foundation of Jiangsu Province, grant number (BK20191096).

Conflicts of Interest: The authors declare no conflict of interest.

References

1. Trumbore, S. Carbon respired by terrestrial ecosystems—Recent progress and challenges. *Glob. Chang. Biol.* **2006**, *12*, 141–153. [CrossRef]
2. Bond-Lamberty, B.; Thomson, A. A global database of soil respiration data. *Biogeosciences* **2010**, *7*, 1915–1926. [CrossRef]
3. Li, H.; Yan, J.; Yue, X.; Wang, M. Significance of soil temperature and moisture for soil respiration in a Chinese mountain area. *Agr. For. Meteorol.* **2008**, *148*, 490–503. [CrossRef]

4. Yan, Z.F.; Bond-Lamberty, B.; Todd-Brown, K.E.; Bailey, V.L.; Li, S.L.; Liu, C.Q.; Liu, C.X. A moisture function of soil heterotrophic respiration that incorporates microscale processes. *Nat. Commun.* **2018**, *9*, 10. [CrossRef] [PubMed]
5. Courtois, E.A.; Stahl, C.; Van den Berge, J.; Bréchet, L.; Van Langenhove, L.; Richter, A.; Urbina, I.; Soong, J.L.; Peñuelas, J.; Janssens, I.A. Spatial Variation of Soil CO_2, CH_4 and N_2O Fluxes Across Topographical Positions in Tropical Forests of the Guiana Shield. *Ecosystems* **2018**, *21*, 1445–1458. [CrossRef]
6. Meyer, N.; Welp, G.; Amelung, W. The Temperature Sensitivity (Q10) of Soil Respiration: Controlling Factors and Spatial Prediction at Regional Scale Based on Environmental Soil Classes. *Glob. Biogeochem. Cycles* **2018**, *32*, 306–323. [CrossRef]
7. Kang, S.Y.; Doh, S.; Lee, D.; Lee, D.; Jin, V.L.; Kimball, J.S. Topographic and climatic controls on soil respiration in six temperate mixed-hardwood forest slopes, Korea. *Glob. Chang. Biol.* **2003**, *9*, 1427–1437. [CrossRef]
8. Zhou, L.; Zhou, X.; Shao, J.; Nie, Y.; He, Y.; Jiang, L.; Wu, Z.; Hosseini Bai, S. Interactive effects of global change factors on soil respiration and its components: A meta-analysis. *Glob. Chang. Biol.* **2016**, *22*, 3157–3169. [CrossRef]
9. Hursh, A.; Ballantyne, A.; Cooper, L.; Maneta, M.; Kimball, J.; Watts, J. The sensitivity of soil respiration to soil temperature, moisture, and carbon supply at the global scale. *Glob. Chang. Biol.* **2017**, *23*, 2090–2103. [CrossRef]
10. Davidson, E.A.; Belk, E.; Boone, R.D. Soil water content and temperature as independent or confounded factors controlling soil respiration in a temperate mixed hardwood forest. *Glob. Chang. Biol.* **1998**, *4*, 217–227. [CrossRef]
11. Liu, Y.; Li, J.; Jin, Y.; Zhang, Y.; Sha, L.; Grace, J.; Song, Q.; Zhou, W.; Chen, A.; Li, P.; et al. The influence of drought strength on soil respiration in a woody savanna ecosystem, southwest China. *Plant Soil* **2018**, *428*, 321–333. [CrossRef]
12. Carey, J.C.; Tang, J.; Templer, P.H.; Kroeger, K.D.; Crowther, T.W.; Burton, A.J.; Dukes, J.S.; Emmett, B.; Frey, S.D.; Heskel, M.A.; et al. Temperature response of soil respiration largely unaltered with experimental warming. *Proc. Natl. Acad. Sci. USA* **2016**, *113*, 13797–13802. [CrossRef] [PubMed]
13. Chen, Z.; Xu, Y.; Zhou, X.; Tang, J.; Kuzyakov, Y.; Yu, H.; Fan, J.; Ding, W. Extreme rainfall and snowfall alter responses of soil respiration to nitrogen fertilization: A 3-year field experiment. *Glob. Chang. Biol.* **2017**, *23*, 3403–3417. [CrossRef] [PubMed]
14. Feng, J.; Wang, J.; Ding, L.; Yao, P.; Qiao, M.; Yao, S. Meta-analyses of the effects of major global change drivers on soil respiration across China. *Atmos. Environ.* **2017**, *150*, 181–186. [CrossRef]
15. Han, C.; Yu, R.; Lu, X.; Duan, L.; Singh, V.P.; Liu, T. Interactive effects of hydrological conditions on soil respiration in China's Horqin sandy land: An example of dune-meadow cascade ecosystem. *Sci. Total Environ.* **2019**, *651*, 3053–3063. [CrossRef]
16. Castellano, M.J.; Schmidt, J.P.; Kaye, J.P.; Walker, C.; Graham, C.B.; Lin, H.; Dell, C. Hydrological controls on heterotrophic soil respiration across an agricultural landscape. *Geoderma* **2011**, *162*, 273–280. [CrossRef]
17. Moyano, F.E.; Manzoni, S.; Chenu, C. Responses of soil heterotrophic respiration to moisture availability: An exploration of processes and models. *Soil Biol. Biochem.* **2013**, *59*, 72–85. [CrossRef]
18. Davidson, E.A.; Verchot, L.V.; Cattanio, J.H.; Ackerman, I.L.; Carvalho, J.E.M. Effects of soil water content on soil respiration in forests and cattle pastures of eastern Amazonia. *Biogeochemistry* **2000**, *48*, 53–69. [CrossRef]
19. Sun, Q.; Wang, R.; Hu, Y.; Yao, L.; Guo, S. Spatial variations of soil respiration and temperature sensitivity along a steep slope of the semiarid Loess Plateau. *PLoS ONE* **2018**, *13*, e0195400. [CrossRef]
20. Sun, B.; Liang, Y.; Xu, R.; Peng, X.; Wang, X.; Zhou, J.; Li, Z.; Zhao, X. Long-term Research on Red Soil Degradation and Remediation Promotes Development of Ecological Recycling Agriculture in Hilly Region of Southeast China. *Bull. Chin. Acad. Sci.* **2018**, *33*, 746–757.
21. Fan, L.C.; Han, W.Y. Soil respiration in Chinese tea gardens: Autotrophic and heterotrophic respiration. *Eur. J. Soil Sci.* **2018**, *69*, 675–684. [CrossRef]
22. Xu, Y.; Shen, Z.H.; Ying, L.X.; Zang, R.G.; Jiang, Y.X. Effects of current climate, paleo-climate, and habitat heterogeneity in determining biogeographical patterns of evergreen broad-leaved woody plants in China. *J. Geogr. Sci.* **2019**, *29*, 1142–1158. [CrossRef]

23. Fu, C.; Zhu, Q.; Yang, G.; Xiao, Q.; Wei, Z.; Xiao, W. Influences of Extreme Weather Conditions on the Carbon Cycles of Bamboo and Tea Ecosystems. *Forests* **2018**, *9*, 629. [CrossRef]
24. Nie, X.F.; Li, H.P.; Jiang, J.H.; Diao, Y.Q.; Li, P.C. Spatiotemporal variation of riverine nutrients in a typical hilly watershed in southeast China using multivariate statistics tools. *J. Mt. Sci.* **2015**, *12*, 983–998. [CrossRef]
25. Yan, P.; Shen, C.; Fan, L.C.; Li, X.; Zhang, L.P.; Zhang, L.; Han, W.Y. Tea planting affects soil acidification and nitrogen and phosphorus distribution in soil. *Agr. Ecosyst. Environ.* **2018**, *254*, 20–25. [CrossRef]
26. Liu, Y.; Zhou, G.; Du, H.; Berninger, F.; Mao, F.; Li, X.; Chen, L.; Cui, L.; Li, Y.; Zhu, D. Soil respiration of a Moso bamboo forest significantly affected by gross ecosystem productivity and leaf area index in an extreme drought event. *PeerJ* **2018**, *6*, e5747. [CrossRef]
27. Hu, S.; Li, Y.; Chang, S.X.; Li, Y.; Yang, W.; Fu, W.; Liu, J.; Jiang, P.; Lin, Z. Soil autotrophic and heterotrophic respiration respond differently to land-use change and variations in environmental factors. *Agr. For. Meteorol.* **2018**, *250–251*, 290–298. [CrossRef]
28. Lai, X.; Zhu, Q.; Zhou, Z.; Liao, K. Influences of sampling size and pattern on the uncertainty of correlation estimation between soil water content and its influencing factors. *J. Hydrol.* **2017**, *555*, 41–50. [CrossRef]
29. Liao, K.; Lai, X.; Zhou, Z.; Zeng, X.; Xie, W.; Castellano, M.J.; Zhu, Q. Whether the Rock Fragment Content Should Be Considered When Investigating Nitrogen Cycle in Stony Soils? *J. Geophys. Res. Biogeosci.* **2019**, *124*, 521–536. [CrossRef]
30. Fan, L.C.; Yang, M.Z.; Han, W.Y. Soil Respiration under Different Land Uses in Eastern China. *PLoS ONE* **2015**, *10*, 18. [CrossRef]
31. Zhu, R.H.; Zheng, Z.C.; Li, T.X.; Zhang, X.Z.; He, S.Q.; Wang, Y.D.; Liu, T.; Li, W. Dynamics of soil organic carbon mineralization in tea plantations converted from farmland at Western Sichuan, China. *PLoS ONE* **2017**, *12*, 14. [CrossRef] [PubMed]
32. Wu, J.J.; Goldberg, S.D.; Mortimer, P.E.; Xu, J.C. Soil respiration under three different land use types in a tropical mountain region of China. *J. Mt. Sci.* **2016**, *13*, 416–423. [CrossRef]
33. Hsieh, I.F.; Kume, T.; Lin, M.Y.; Cheng, C.H.; Miki, T. Characteristics of soil CO_2 efflux under an invasive species, Moso bamboo, in forests of central Taiwan. *Trees* **2016**, *30*, 1749–1759. [CrossRef]
34. Sheng, H.; Yang, Y.; Yang, Z.; Chen, G.; Xie, J.; Guo, J.; Zou, S. The dynamic response of soil respiration to land-use changes in subtropical China. *Glob. Chang. Biol.* **2010**, *16*, 1107–1121. [CrossRef]
35. Sun, Q.; Wang, R.; Wang, Y.; Du, L.; Zhao, M.; Gao, X.; Hu, Y.; Guo, S. Temperature sensitivity of soil respiration to nitrogen and phosphorous fertilization: Does soil initial fertility matter? *Geoderma* **2018**, *325*, 172–182. [CrossRef]
36. Mahal, N.K.; Osterholz, W.R.; Miguez, F.E.; Poffenbarger, H.J.; Sawyer, J.E.; Olk, D.C.; Archontoulis, S.V.; Castellano, M.J. Nitrogen Fertilizer Suppresses Mineralization of Soil Organic Matter in Maize Agroecosystems. *Front. Ecol. Evol.* **2019**, *7*, 59. [CrossRef]
37. Flanagan, L.B.; Johnson, B.G. Interacting effects of temperature, soil moisture and plant biomass production on ecosystem respiration in a northern temperate grassland. *Agric. For. Meteorol.* **2005**, *130*, 237–253. [CrossRef]
38. Zhou, W.P.; Hui, D.F.; Shen, W.J. Effects of Soil Moisture on the Temperature Sensitivity of Soil Heterotrophic Respiration: A Laboratory Incubation Study. *PLoS ONE* **2014**, *9*, 10. [CrossRef]
39. Chen, H.; Zou, J.; Cui, J.; Nie, M.; Fang, C. Wetland drying increases the temperature sensitivity of soil respiration. *Soil Biol. Biochem.* **2018**, *120*, 24–27. [CrossRef]
40. Fang, C.; Moncrieff, J.B. The dependence of soil CO2 efflux on temperature. *Soil Biol. Biochem.* **2001**, *33*, 155–165. [CrossRef]
41. Wang, W.J.; Dalal, R.C.; Moody, P.W.; Smith, C.J. Relationships of soil respiration to microbial biomass, substrate availability and clay content. *Soil Biol. Biochem.* **2003**, *35*, 273–284. [CrossRef]
42. Yu, C.Q.; Wang, J.W.; Shen, Z.X.; Fu, G. Effects of experimental warming and increased precipitation on soil respiration in an alpine meadow in the Northern Tibetan Plateau. *Sci. Total Environ.* **2019**, *647*, 1490–1497. [CrossRef] [PubMed]
43. Joshi, C.; Mohanty, B.P.; Jacobs, J.M.; Ines, A.V.M. Spatiotemporal analyses of soil moisture from point to footprint scale in two different hydroclimatic regions. *Water Resour. Res.* **2011**, *47*. [CrossRef]

44. Western, A.W.; Grayson, R.B.; Bloschl, G.; Willgoose, G.R.; McMahon, T.A. Observed spatial organization of soil moisture and its relation to terrain indices. *Water Resour. Res.* **1999**, *35*, 797–810. [CrossRef]
45. Foley, J.A.; DeFries, R.; Asner, G.P.; Barford, C.; Bonan, G.; Carpenter, S.R.; Chapin, F.S.; Coe, M.T.; Daily, G.C.; Gibbs, H.K.; et al. Global consequences of land use. *Science* **2005**, *309*, 570–574. [CrossRef]